

LARGE EDDY SIMULATION OF THE FLOW IN A BLADED DIFFUSER

Doru Caraeni* Stephen Conway†
Laszlo Fuchs‡

Dept. of Heat and Power Engineering, Fluid Mechanics,
Lund Institute of Technology, SE-221 00 Lund, Sweden

12-15 September 1999

ABSTRACT

The advances made in computer technology over recent years have lead to a great increase in the engineering problems which can be simulated using CFD. The computation of flows over complex geometries at relatively high Reynolds number is becoming more common using Large Eddy Simulations (LES), as recent reviews on the subject have shown (Piomelli, 98). Direct Numerical Simulations (DNS) of such flows is still beyond the capacity of today's largest supercomputers, requiring many millions of computational cells and excessive computational times. In addition, traditional Reynolds Averaged Navier-Stokes (RANS) methods fail for various reasons for many of the industrial applications of interest. In an increasing number of cases LES is seen as the only real alternative.

The anisotropic dynamic SGS models (Abba) have the potential of yielding better performances, for wall bounded flows. In this study, the Dynamic Divergence Model (DDM) has been used. It is a novel anisotropic dynamic SGS model (Held, 1998) (Conway, 1998) , with independently determined coefficients in each direction. It has been designed to allow anisotropy, for wall bounded flows. Some results for the classical turbulent channel flow, while using DDM, are presented. The results obtained compare well with the experimental and DNS data.

LES has been used to solve the flow through a bladed diffuser positioned at the inlet to a gas turbine combus-

tion chamber. Flows through such geometries at high Reynolds number are inherently time dependent, involve transition to and development of turbulence, fully three dimensional boundary layers, separation, etc. A simplified geometry has been studied previously (Conway, 1998). This work covers the next stage in the study. A new flow solver has been used in the present calculations. ParNAS3D¹ is a parallel Navier-Stokes solver, that has been developed at LTH² for simulations of engineering turbulent compressible flows, using LES.

NUMERICAL ALGORITHM

The ParNAS3D algorithm is based on the Residual Distribution Schemes approach and it has a better accuracy of the solution if we compare with the classical upwind finite-volume formulations, (Wood, 1998). It works on an originally developed cell-vertex data structure, for unstructured meshes (Mitran, 1997). The program uses a multidimensional-upwind, system distribution scheme, for the inviscid part of the Navier Stokes equations, while a central Galerkin finite-element procedure is employed for the diffusive part (Paillere, 1997) (Deconinck, 1997) and for the unstationary term. The time integration is performed using an implicit, Jameson-type scheme (dual time stepping). To accelerate the convergence of the solution at each real-time step, multigrid iterations are performed.

The update scheme for the unstationary Navier Stokes equations is:

*Ph.D. Student, LTH, Sweden, dc@ms.vok.lth.se

†Ph.D. Student, LTH, Sweden, scon@ms.vok.lth.se

‡Professor, LTH, Sweden, lf@ms.vok.lth.se

¹Parallel Numerical Aeronautical Simulations 3D

²Lund Institute of Technology

$$U^{n+1} = U^n - \frac{\Delta\tau}{V_i} \left\{ \sum_{T \in \Omega_i} [\beta_i^T \phi_{inviscid}^T + \frac{1}{3}(F_j^v n_{j,i})] - \sum_{T \in \Omega_i} \frac{1}{4} V_T [\frac{\partial U}{\partial t}]_{implicit}^{(T \cap \Omega_i)} \right\} \quad (1)$$

where:

$U = (\rho, \rho u_1, \rho u_2, \rho u_3, \rho E,)$ is the conservative variables vector, $\Delta\tau$ is the local (pseudo-) time step, T is one of the cells (tetrahedral) sharing the node, V_i is the volume of the dual cell Ω_i around the node i ($V_i = \sum_{T \in \Omega_i} \frac{1}{4} V_T$), $\beta_i^T \phi_{inviscid}^T$ is the contribution of the advective part of the Navier-Stokes eqns., β_i^T is the upwind matrix-distribution coefficient for the convective term and $\phi_{inviscid}^T$ the advective-residual over the cell T , i.e. :

$$\phi^T = \int \int_T \text{div}(F^c) d\Omega \quad (2)$$

F^c is the advective flux, $\frac{1}{3}(F_j^v n_{j,i})$, the contribution of the viscous forces (central-Galerkin) where F^v is the viscous flux, and $[\frac{\partial U}{\partial t}]_{implicit}^{(T \cap \Omega_i)}$ is the average of $[\frac{\partial U}{\partial t}]_{implicit}$ on $(T \cap \Omega_i)$, i.e. the contribution of the unstationary term. The flow solver is second order accurate in both space and time, and it has been used for LES of flows in industrial applications (Caraeni, 1999).

DYNAMIC DIVERGENCE MODEL

The Smagorinsky model, Lilly's Dynamic Model (Lilly, 1991) and the DDM model have been implemented in the ParNAS3D code. While the Smagorinsky and Lilly's models are well known and have been used in a large number of LES computations, the DDM is a novel, anisotropic dynamic SGS model, with independently determined coefficients in each direction. Dynamic SGS models (with one model-parameter) normally require to use some projection method to contract the tensorial relation for the model parameter. Germano (Germano, 1991) contracted the tensorial relation with the large scales strain rate tensor and had to average in homogeneous directions in order to ensure the numerical stability of the model. Lilly (Lilly, 1991) proposed a least square minimization procedure. Models with only one model parameter implicitly assume small scale isotropy. This requires that the flow field should be well resolved and that sources of anisotropy, e.g. walls and stagnation points, are absent. Since the small scale turbulence tends to isotropy (in contrast to the large scale eddies) high spatial resolution is a

pre-requisite for such SGS models. This requirement can be a serious limitation when computing the flow in wall bounded problems, because of the large number of grid points required close to the solid boundary. Recently, dynamic SGS models with more than one model-parameter have been developed and used with success for LES simulations (Abba). The DDM model has been designed to remedy the anisotropy problem mentioned above, in a simple manner. Since in the governing equation one encounters only the divergence of the sub-grid scales stress tensor, we can compute these independently. Lets consider the resolved turbulent stress tensor L_{ij} :

$$L_{ij} = -\widehat{\bar{\rho}}(\widehat{u_i u_j} - \widehat{u_i} \widehat{u_j}) \quad (3)$$

This quantity can be directly computed. Using Germano's identity yields:

$$L_{ij} = T_{ij} - \widehat{\tau}_{ij} \quad (4)$$

where

$$T_{ij} = -\widehat{\bar{\rho}}(\widehat{u_i u_j} - \widehat{u_i} \widehat{u_j}) \quad (5)$$

is the subtest-filter scale stress tensor and

$$\tau_{ij} = -\bar{\rho}(\widetilde{u_i u_j} - \widetilde{u_i} \widetilde{u_j}) \quad (6)$$

is the subgrid scales stress tensor, τ_{ij} , which has to be filtered (at the test filter level). The divergence of the SGS stress tensor and sub-test filter stress tensor are modelled by taking the divergence of the compressible generalization of the Smagorinsky expression:

$$\tau_{ij,j} = C^{(i)} [2\Delta^2 \bar{\rho} \Pi_S^{1/2} (\widetilde{S}_{ij} - \frac{1}{3} \widetilde{S}_{kk} \delta_{ij})]_{,j} \quad (7)$$

$$\tau_{ij,j} = C^{(i)} \alpha_{ij,j} \quad (8)$$

$$T_{ij,j} = C^{(i)} [2\widehat{\Delta}^2 \widehat{\bar{\rho}} \Pi_S^{1/2} (\widehat{S}_{ij} - \frac{1}{3} \widehat{S}_{kk} \delta_{ij})]_{,j} \quad (9)$$

$$T_{ij,j} = C^{(i)} \beta_{ij,j} \quad (10)$$

[Note that there is no summation on the index i].

$$\widetilde{S}_{ij} = \frac{1}{2} (\frac{\partial \widetilde{u_i}}{\partial x_j} + \frac{\partial \widetilde{u_j}}{\partial x_i}) \quad (11)$$

$$\Pi_{\tilde{S}} = 2(\tilde{S}_{mn}\tilde{S}_{mn}) \quad (12)$$

Hence the three model parameters $C^{(i)}$ can be calculated independently as,

$$C^{(i)} = \frac{L_{ij,j}}{\beta_{ik,k} - \alpha_{il,l}} \quad (13)$$

These model parameters are calculated dynamically at each point from the instantaneous flow field. A bound based on the Reynolds number and local space average on the model parameters avoids numerical stability problems, (Olsson, 1998). Negative values of $C^{(i)}$ enable back-scatter, which implies that turbulent energy can be transferred (intermittently) from the small scales to the larger ones.

PARALLEL ALGORITHM

Large Eddy Simulations for engineering applications are typically extremely expensive, requiring huge resources (in terms of processor power and memory) and long computational times. When using large parallel computations, LES becomes accessible for many industrial applications. The ParNAS3D code uses PVM for message passing, therefore it can run as well on large distributed memory machines (Cray T3E, IBM SP2...), on the SGI Origin 2000 servers or on a heterogeneous collection of platforms. The parallelization of the code has been done using the SPMD (Single Program Multiple Data) paradigm.

RESULTS

Parallel Results

The ParNAS3D code has been run on an SGI Origin 2000 platform, on up to 8 processors, and also on a cluster of 2 WinNT PC's, using an Ethernet connection. The results, addressing the parallel speed-up are presented graphically in Fig.1. It can be seen that the performance, when using the two WinNT PC cluster, has been close to 75%, due to poor communication while using the Ethernet connection. The code proved instead to have excellent scalability, on the Origin platform (95-98%).

Channel Flow Results

First, the results for the classical turbulent channel flow are presented. The Reynolds number based on the bulk velocity and the channel height, is 5800. No-slip

isothermal boundary conditions have been set at the walls, while periodicity boundary conditions have been used both in the streamwise (x) and the spanwise (z) directions. Computations have been performed using the dynamic DDM model. The grid size is $2\pi\delta \times \delta \times (2\pi/3)\delta$ where δ is the channel height. The grid has $85 \times 51 \times 51$ nodes and approx. 1,240,000 tetrahedral cells. The grid is stretched in the y -direction ($y^i = \delta \sin(\rho_i)$, for $\rho_i = \pi/2 * (j-1)/(N-1)$, $j = 1, 2, \dots, N$. Here N is the number of grid points in the y -direction), but uniform in the streamwise and the spanwise directions. The flow has been simulated for enough flow-through times (the domain length in the streamwise direction divided by the bulk velocity) to get a statistically stationary turbulent channel flow. Data for statistics are accumulated over the last 15 flow-through times. Planar averages are calculated by averaging for all points on planes parallel to the walls and in time, and the results are presented as a function of wall-distance (y) only, and compared with experiments (Kreplin, 1979) and with DNS data (Kim, 1987). The averaged non-dimensional friction velocity $\bar{u}_\tau = 0.06156$ (i.e. u_τ/U_b , where U_b is the bulk velocity) compares well with the DNS and the experimental (i.e. $\bar{u}_\tau = 0.0643$) result. Figures 2...5 show planar averaged time averages of the mean of the axial velocity and Root-Mean-Square of velocity fluctuations (RMS of Favre U'' , V'' , W''). The results are normalized using the friction velocity, u_τ . The results obtained using the DDM model compare well with the DNS and the experimental results.

Bladed-Diffuser Results

The bladed diffuser forms part of the fuel injection system of an industrial gas turbine. The diffuser is mounted radially on the fuel injector. Its roll is to induce swirl into the primary air flowing into the combustion chamber and hence enhance fuel air mixing. A cylindrical gaseous fuel injector is placed slightly upstream of the blade cascade. It was found that under certain operating conditions when increasing the blade incidence angle, the turbine started to vibrate and that the production of NO_x increased substantially. These phenomena are probably caused by a non-stationary flow field and vortex shedding which develops due to flow separation at these high angles. The vibrations are more than likely a result of the non-stationary pressure field and the increase in NO_x is a result of poor mixing

of the fuel and air. It is therefore interesting to study this problem both because of the complex flow features and because it fits very well into the range of engineering applications which can be studied using LES. Only a 15 degree segment of the diffuser was modelled.

The results presented here are from our simulations using the DDM model. The LES computations have been carried out on a grid of about 950,000 cells, using up to 8 processors. These simulations give us a good insight into this complex flow problem. The Reynolds number, based on the bulk inlet velocity U_{in} and the chord length of the blade, is 16,000. Grid clustering together with the van Driest's damping function, to modify the model coefficients, have been used at the walls. Fig.6 shows isocontours of Mach number. The results are shown for a cross section of the geometry normal to the cylinder axis and are averaged in time (4096 time steps). We can see that a large region of separation develops behind the cylinder, creating a blockage effect at the inlet to the diffuser blade cascade. On the pressure side of the blade, separation occurs very early and a large region of recirculating flow develops. This flow reattaches near the trailing edge. On the suction side separation occurs at roughly 40% chordlength, a turbulent boundary layer develops and vortices are shed from the trailing edge of the blade. The blocking effect of the cylinder causes the point of maximum Mach number to move backwards along the blade surface. An increase in velocity near the trailing edge is created by the dual effect of the developing boundary layer and cylinder wake. The cylinder wake is seen to be less pronounced than expected, due to the suction effect within the blade passage. The regions where the turbulent fluctuations attain high levels are depicted in Fig. 7, in terms of Root Mean Square of the fluctuations of the Mach number. Fig. 8 presents the mean skin-friction $\bar{\tau}_w$ at the blade surface on the suction side, non-dimensionalized by using the diffuser's inlet dynamic pressure ($\rho_{in}U_{in}^2/2$), i.e. a friction coefficient, C_f . It shows a large separated boundary layer region ($C_f < 0$). This separation is the result of the high adverse pressure gradient (at 40-45% chord-length from the leading edge) on the airfoil suction side. Fig. 9 shows the high levels of the pressure fluctuations in the separated boundary layer region on the suction side of the airfoil, in terms of Root Mean Square of pressure fluctuations (non-dimensionalized by using $\rho_{in}U_{in}^2/2$). On the pressure side of the blade a

similar phenomenon occurs. Due to the large curvature of the blade close to the leading edge, the flow accelerates, and shortly after decelerates creating an adverse pressure gradient, leading to flow separation. Close to the trailing edge the flow reattaches again. Fig. 10 shows the power spectral density of the turbulence kinetic energy in the wake of the blade cascade. It proves the temporal behavior of the flow, including the presence of coherent structures with well defined frequencies. The results obtained from these LES computations recover Kolmogorov's theoretical $-5/3$ decay of the turbulent kinetic energy for homogeneous turbulence. The range of the $-5/3$ interval is limited by grid resolution and anisotropic effects of the solid walls. The results show that vortices are shed with a definite frequency of approx. 2 kHz. It is interesting to note that the similar frequencies are obtained in the cylinder wake. Most probably the flow across the cylinder influences the flow in the blade passage. Notably it affects the flow in the separated boundary layer, on the suction side. Similar spectra results are obtained when using the implicit SGS model, but the inertial sub-range is not so well reproduced. Thus, it is clear that the introduction of a dynamic SGS model improved the accuracy of our simulations.

CONCLUSIONS

Large Eddy Simulations of the flow across a bladed diffuser have been carried out using the DDM model. In the near future, computations using some other dynamic SGS models may be considered, to estimate the effect these have on the results from an engineering point of view (mean values, shedding frequencies, rms of fluctuations, etc.). These simulations give us a good insight into this complex flow problem and it is hoped that they will be beneficial to the design of the future diffusers.

ACKNOWLEDGEMENTS

Computer resources from LUNARC at Lund University are gratefully acknowledged.

REFERENCES

- A.Abbas, C.Cercignani, L. Valdetaro, P. Zanini, "LES of turbulent thermal convection", Direct and Large Eddy Simulation II, Luwer Academic Publisher, pp 147-156.

S. Conway, L. Fuchs, "Investigation of the Flow Across a Swirl Generator using LES", AIAA 98-0921, Reno 1998.

H. Deconinck, R. Struijs, G. Bourgois, P.L. Roe, "High resolution shock capturing cell vertex advection schemes on unstructured grids", VKI Lecture Series, March 21-25, 1994.

D. Caraeni, C. Bergstrom, L. Fuchs. "Parallel NAS3D: An Efficient Algorithm for Engineering Spray Simulation Using LES", 23-26 May, International Parallel CFD 1999 Conf., Williamsburg, USA.

D. Caraeni, C. Bergstrom, L. Fuchs. "LES of Spray in Compressible Flows on Unstructured Grids", ASME-CFD Conf. 1-5 Aug. 1999, Boston, USA.

J. Held, L. Fuchs, "Large Eddy Simulation of Separated Transonic Flows around a Wing Section", AIAA 98-0405, Reno 1998.

U. Piomelli, "Large-Eddy Simulation: Present State and Future Directions", AIAA 98-0534.

M. Germano, P. Piomelli, P. Moin, W.H. Cabot, "A dynamic subgrid-scale eddy viscosity model", Phys. Fluids A, 3:1760-1765, 1991.

H. Kreplin and H. Eckelmann. "Behavior of the Three Fluctuating Velocity Components in the Wall Region of a Turbulent Channel Flow". Physics of Fluids. 22(7): 1233-1239, 1979.

J. Kim, P. Moin, and R. Moser. "Turbulence Statistics in Fully Developed Channel Flow at Low Reynolds Number". Journal of Fluid Mechanics, 177: 133-166, 1987

D.K. Lilly, "A proposed modification of the Germano subgrid-scale closure method", Phys. Fluids A, 4:633-635, 1991.

S. Mitran, D. Caraeni, D. Livescu, "Large Eddy Simulation of Rotor Stator interaction in Centrifugal Impeller", JPC, Seattle, July 1997.

M. Olsson, L. Fuchs, "Large eddy simulation of a forced semiconfined circular impinging jet", Physics of Fluids, V. 10, 1998.

H. Paillere, H. Deconinck, E. van der Weide, "Upwind Residual Distribution methods for compressible flows: An alternative for Finite Volume and Finite Element methods", VKI 28th CFD Lecture Series, March 1997.

William A. Wood, William L. Kleb, "Diffusion Characteristics of Upwind Schemes On Unstructured Triangulations", AIAA 98-2443, Albuquerque, NM 1998.

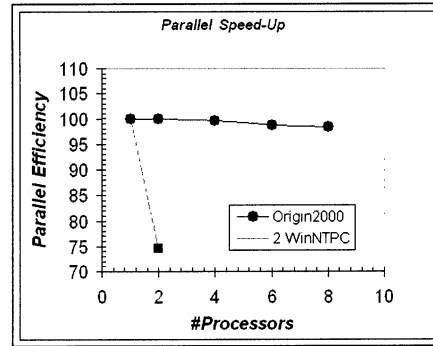


Fig. 1 Parallel scalability of ParNAS3D

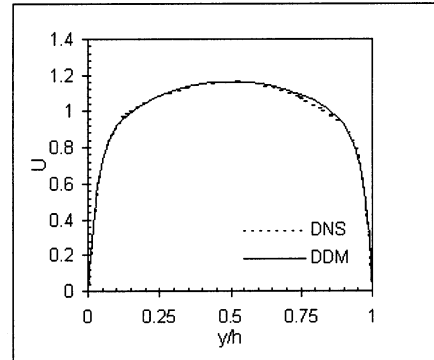


Fig. 2 Planar Time Averages of Velocity U

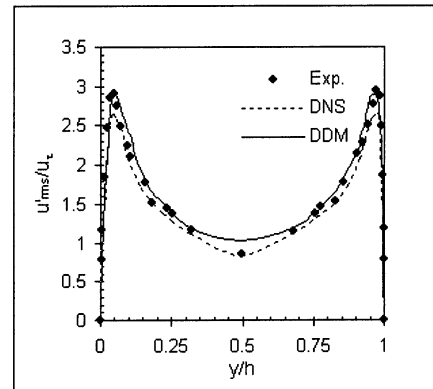


Fig. 3 Planar Averages of U_{rms}

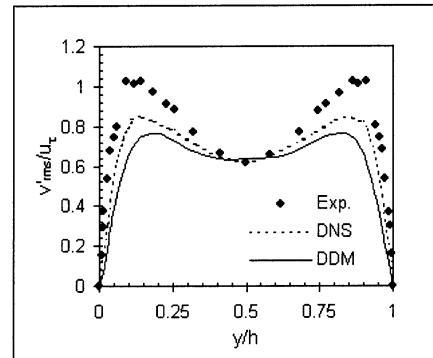


Fig. 4 Planar Averages of V_{rms}

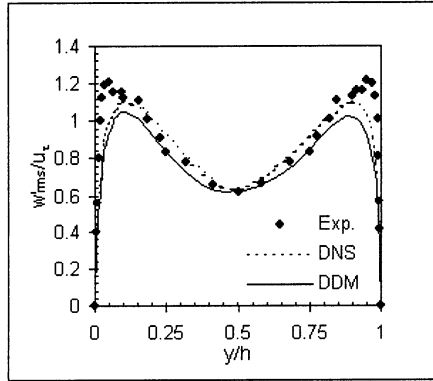


Fig. 5 Planar Averages of W''_{rms}

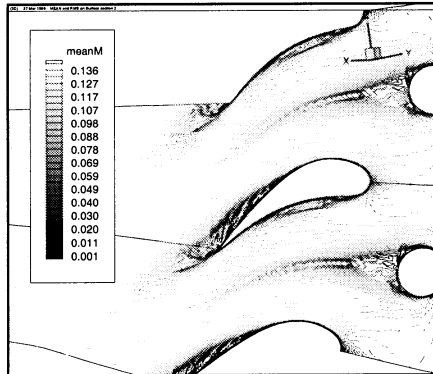


Fig. 6 Distribution of mean Mach number

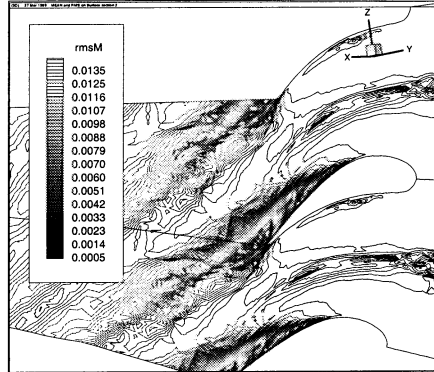


Fig. 7 Distribution of RMS of Mach number

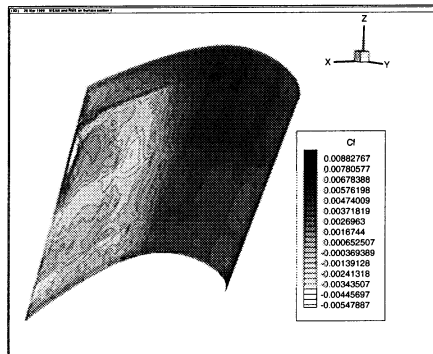


Fig. 8 Distribution of mean skin-friction

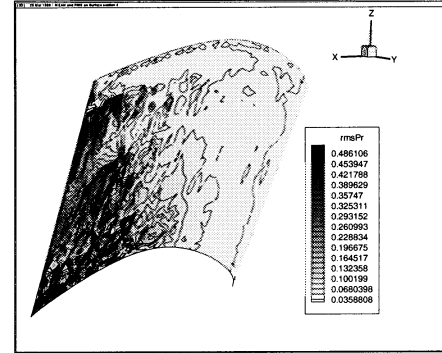


Fig. 9 Distribution of RMS of pressure

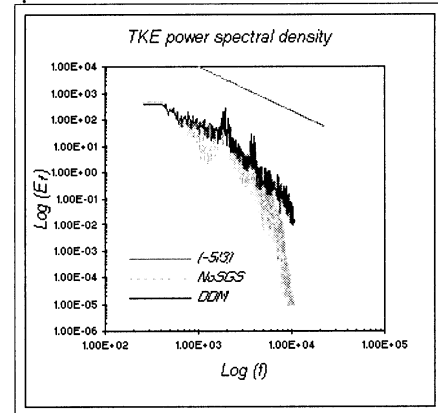


Fig. 10 Spectra of Turbulent Kinetic Energy